Electronic interactions between gold nanoclusters in constrained geometries

Sang Hoon Kim,[1] S. Hwang,[2] Young-Seok Shon,[2] D. Frank Ogletree,[1] and Miquel Salmeron[1,*]
[1]*Materials Sciences Division, Lawrence Berkeley National Laboratory, University of California, Berkeley, California 94720, USA*
[2]*Department of Chemistry, Western Kentucky University, Bowling Green, Kentucky 42101, USA*
(Received 9 December 2005; published 6 April 2006)

The interactions between gold nanoclusters dispersed in decane ($C_{10}H_{22}$) when confined in narrow gaps of a few nanometers were investigated. The diameter of the gold core was 1.8 nm. The clusters were capped off with alkanethiol molecules of different lengths (C_6S and $C_{15}S$) to prevent metallic contact with each other. By applying force to the gap walls, the cluster suspension was squeezed out of the gap in a nearly continuous way. In the case of the shorter ligand C_6S, the width of the minimum gap at the highest applied force was 7 nm (~3 cluster diameters). In contrast with the continuous decrease in thickness, the gap capacitance exhibited stepwise increases, which are interpreted as Mott type insulator-to-metal transition of aggregates of clusters under pressure when the average distance between the metallic cores becomes less than ~1 nm. With longer ligands, $C_{15}S$, the thickness of the minimum gap was 12–15 nm. In that case, no discontinuous steps in thickness or capacitance were observed, showing that the longer ligand effectively prevents exchange interactions between the metallic cores of the nanoclusters.

DOI: 10.1103/PhysRevB.73.155406 PACS number(s): 31.10.+z

I. INTRODUCTION

Nanometer size metal clusters containing several hundred atoms are attracting interest due to their size-dependent electronic and magnetic properties.[1–3] Such unique properties are due to their large surface/volume ratio and to quantum size effects.[4,5] A large fraction of surface atoms can change their electronic structure because of the different *d*- and *s*-orbital hybridization of the surface and bulk atoms. Quantum size effects give rise to increased spacing between energy levels and eventually to the formation of energy gaps when the size becomes small enough, in effect changing from metallic to insulating.

Metallic nanoclusters are difficult to isolate due to their high surface energy, easily forming aggregates rather than staying separated. Therefore nanoclusters synthesized by wet chemistry methods need to be stabilized by organic ligand molecules. The ligands themselves may alter the electronic and magnetic properties of the nanoclusters due to the charge transfer between metallic core and ligands.[3,6,7]

In addition to investigating the properties of individual clusters, it is crucial to understand the interactions between clusters and between the clusters and substrate if they are to be used as building blocks for more complex structures[8,9] or in biological applications.[10] Morphological and structural analysis of nanocrystal superlattices formed after solvents evaporation have been performed with TEM, and x-ray scattering, and diffraction.[11,12] Optical[13] and impedance[14] spectroscopy and SQUID magnetometry[15] of Langmuir monolayers of metallic nanoclusters consistently showed Mott type insulator-to-metal transitions as a function of interparticle distance. Recently, x-ray photoemission spectroscopies on aggregates of gold nanoclusters showed significant cross-coupling between nanoclusters when their separation decreased below 1 nm.[16] In contrast to the interactions in aggregates or superlattices of nanoclusters, little is known about the interactions between nanoclusters in suspension.[11] In this paper we report our investigations of such interaction by studying the mechanical and dielectric response of gold nanoclusters dispersed in an organic solvent under pressure in a confined geometry.

II. EXPERIMENTAL

A Surface Force Apparatus (SFA) was used to produce a gap between two atomically flat and parallel mica surfaces. The gap separation can be controlled with angstrom precision. Traditionally the SFA has been used to study the mechanical response of thin liquid films in the gap.[17] Our home-built SFA was described previously in detail.[18] Briefly two thin mica sheets are glued onto 2 cm diameter cylindrical lenses with a crossed axis. One lens is mounted on a cantilever beam along with a magnet. To ensure that the mica surfaces are free of contamination, they are cleaved after cutting and mounting, just before insertion of the liquid.[19,20] Loads are applied to the cantilever to approach the two mica surfaces by means of a magnetic field produced by passing an electric current through Helmholtz coils. To measure the distance between the mica surfaces, thin silver films (~60 nm) are evaporated on the backside of the mica sheets. White light from a slit passes through the lenses and produces interference fringes that are used to calculate the distance between the silver mirrors. The combined thickness of the mica sheets is first measured in dry contact. After that, the surfaces are pulled apart and liquid is injected in between.[21] When the mica surfaces are in contact or when the confined material can sustain a load, elastic deformation of the mica occurs. This produces a confined region that is parallel and atomically flat. The diameter of this contact area can be measured from the interference fringes shape.

The dielectric response of the confined sample is studied by measuring the capacitance between the two silver mirrors on the back sides of the mica sheets, as described previously.[22] The sensitivity of the measurement depends primarily on the thickness of the mica substrates.[23] Changes

as small as 0.1 fF can be measured using a 60 kHz ac capacitance bridge. A container with P_2O_5 desiccant placed inside the SFA chamber maintained low humidity during experiments.[24]

In previous designs of SFA, data acquisition and processing of interference fringe images was slow and tedious. First the fringes were recorded with a CCD camera onto a VCR cassette tape and then transferred to a computer. The typical time to collect and analyze a fringe image was 30 s,[23] limiting the time resolution for a measurement of the thickness profile of the sample liquid. On the other hand, capacitance measurements can be made in milliseconds.[23] A new software/hardware system was developed that made it possible to record fringe images directly into the computer with a real-time analysis of the fringe positions while simultaneously recording the capacitance data. Thickness and capacitance changes for confined samples could thus be measured with 100 ms time resolution.

The gold nanoclusters used in this study had a diameter of 1.8 nm and were stabilized by alkanethiols of two different chain lengths: hexanethiol (C_6S) and pentadecanethiol ($C_{15}S$).[16] Synthesis was performed using the Brust reaction, where $AuCl_4^-$ is transferred to toluene using tetraoctylammonium bromide. The addition of alkanethiols followed by a reduction with $NaBH_4$ generated alkanethiolate-protected gold nanoclusters.[25] The nanoclusters were dispersed in decane ($C_{10}H_{22}$) at a concentration of 3.5 mM, near the solubility limit, with a nanoparticle concentration of ~3% by volume. At a higher concentration, it was difficult to maintain dispersion, and large aggregates, ten to a hundred nanometers in size, formed. These aggregates were incompatible with SFA experiments.

The experiments were performed by linearly increasing the force applied to the cantilever supporting one of the mica samples. When the two surfaces are far apart, the force deflects the cantilever and reduces the separation between the surfaces at a constant rate. In the experiments reported here an approach speed of ~1 nm/s, was applied. This was sufficiently slow for viscous forces to be negligible. As the surfaces come to contact, the relative motion of the mica samples almost stops, and a flat contact is created with liquid trapped in the gap. In the absence of significant adhesion between the surfaces, the contact can be described by the Hertz model and its diameter increases as the cube root of the applied load.

Before presenting the experimental results, we will briefly discuss the calculation of the capacitance. The capacitance between two cylinders can be approximated by that of a sphere and a flat surface when their separation is small compared to the radius of the sphere or cylinders. In this case the capacitance is given by

$$C_{sphere}(d) \approx 2\pi R\varepsilon_0\varepsilon_f\left(\log\frac{\varepsilon_m R}{\varepsilon_m d+\varepsilon_f D}+k_1\right),$$

$$\frac{\partial C_{sphere}}{\partial d}(d) \approx -2\pi\varepsilon_0\varepsilon_m\frac{R}{D}, \tag{1}$$

where R is the radius of curvature of the mica sheets; D is the combined thickness of the mica sheets, d is the separation between the sheets; ε_m and ε_f are the dielectric constants of mica (ε_m=7) and the fluid; k_1 is a constant of order unity. In our case $R \gg D \gg d$. The expression above was obtained using the method described in Ref. 22 and explicitly taking the dielectric constants of the two materials into account. Typically the distance between the silver electrodes is ~5 μm and d is less than 30 nm, which gives a total capacitance of ~14 pF. The rate of change of capacitance with separation d is ~−0.8 fF/nm.

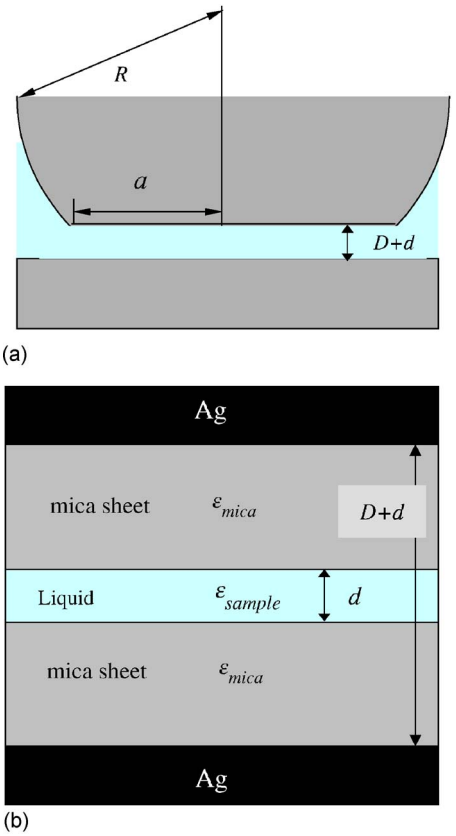

FIG. 1. (Color online) (a) Schematic diagram showing the geometry of the contact between crossed cylindrical lenses. (b) Detail of the contact region.

When a flat contact area of radius a is produced by elastic deformation of the cylinders, the capacitance outside the contact is still given by $C_{sphere}(d)$ to first order in a/R, since the effect of removing the spherical cap is compensated by the small reduction of $a^2/2R$ in average separation. The additional contribution from the flat contact region [Fig 1(a)] is

$$C_{contact}(a,d)=\frac{\pi\varepsilon_0\varepsilon_m\varepsilon_f a^2}{\varepsilon_m d+\varepsilon_f D}, \quad \frac{\partial C_{contact}}{\partial d}(a,d)\approx -\frac{\pi\varepsilon_0\varepsilon_m^2 a^2}{\varepsilon_f D^2}. \tag{2}$$

For a contact radius of 25 μm, C_{contact}~24 fF, and the rate of change with d is ~−0.014 fF/nm. Without liquid inserted, the separation d in contact will be zero, however, when fluid is present the separation d will generally be a function of the average contact pressure. If d is constant, then the total capacitance will increase as the two-thirds power of the applied load, proportional to the increase in

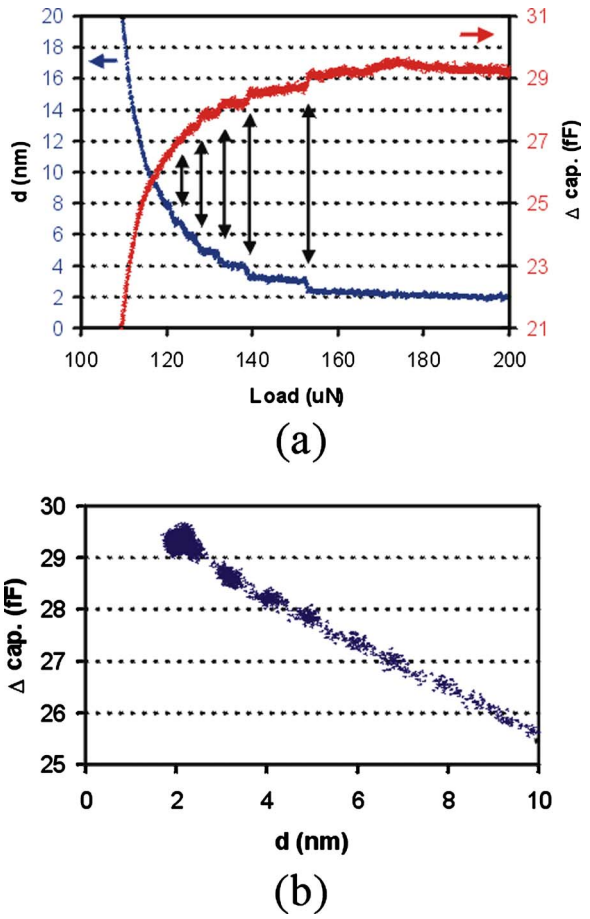

FIG. 2. (Color online) (a) Force-distance and force-capacitance curves for OMCTS, a nonpolar liquid of 0.9 nm diameter molecules. The steps in the *f-d* and *f-c* curves are due to layering transitions in OMCTS. (b) Distance-capacitance change curve from (a). There is a 1:1 correspondence between steps in the *f-d* and *f-c* curves, so the *d-c* curve is linear.

contact area. We can measure a and hence $C_{contact}$ from the shape of the interference fringes.

Once the surfaces make contact, two factors contribute to changes in the capacitance. The first is due to the increasing Hertzian contact area with load; the second and more interesting factor is the change due to pressure-dependent changes in d. The capacitance data presented later has been corrected for load-dependent changes in the Hertzian contact area, to focus on the scientifically interesting changes.[22]

III. RESULTS

We will first show results for octamethyltetrasiloxane (OMCTS), whose behavior is well known in SFA experiments. OMCTS is a nonpolar liquid made of quasispherical molecules 0.9 nm in diameter.[26] At large gap widths, expulsion of the liquid produces a smooth separation versus force curve. Step-wise increases in force, however, are measurable when the gap width is below 6 to 10 molecular diameters.[26] Figure 2(a) shows the measured gap distance and capacitance variations with a linearly increasing applied load. An approach speed of ~1 nm/s was chosen to minimize instrumental drifts and hydrodynamic force.[27] Down to about 14 nm the decrease in gap separation takes place at a constant rate, showing liquid behavior. Below 14 nm, the change in separation slows as the molecules start to order and resist the applied load. Below about 8 nm, changes in separation occur in discrete steps, down to 2 nm. The step size is about 1 nm, the diameter of the OMCTS molecule. The last 2 nm of confined OMCTS could not be expelled, indicating that 2 monolayers of OMCTS remain adsorbed, one bound to each mica surface.[28]

The capacitance, measured simultaneously, increases as the separation decreases. Above 14 nm the increase is linear. Below 8 nm the rate of increase slows and shows discrete steps of about 0.5 fF correlated with the stepwise decreases in separation. Figure 2(b) shows the distance-capacitance (d-c) curve. It is a linear relation, as expected. Below about 8 nm, the curve breaks into discrete segments due to stepwise changes of distance and capacitance. This correlation between thickness and capacitance is due to the fact that OMCTS is a nonpolar dielectric material, and its electronic properties remain unchanged during confinement. The decrease in distance between electrodes alone contributes to the increases in capacitance.

We can estimate the size of the capacitance steps from Eqs. (1) and (2). The dielectric constant of the fluid ε_{OMCTS} is 2.4. We assume that the contact area remains constant when a layer of OMCTS is expelled. (No change was observed in the shape of the fringes within a lateral resolution of a few microns). Referring to Fig 1, the mica thickness D was 5.015 μm and the contact radius $a=15$ μm, so that a change Δd of 1 nm should produce $\Delta C \sim 0.78$ fF, which roughly corresponds to the experimental value, 0.5 fF.

Experiments were then performed on decane suspensions of Au nanoparticles capped by short (C_6S, 0.8 nm) or long ($C_{15}S$, 2.0 nm) alkanethiol ligands, as well as pure decane. In both cases the suspension concentration was 3.5 mM, or approximately one particle per 8 nm^3. The diameter of the Au core was 1.8 nm. The effective diameter of the particles (core+ligand) is not known, since we do not know the detailed conformation of the ligand molecules in solution. The particles will have the maximum diameter $D_{max}=d_{core}+2L$, where L is the length of the molecule, if the ligand alkyl chains are fully extended, presumably with decane solvent molecules intercalated into the ligand shell. The particles will have a smaller effective diameter if the chains tilt or wrap around the core to maximize the van der Waals interactions with each other and the core. On flat Au(111), the alkanethiols molecules are straight and tilted ~30° from the surface normal, so for a gold substrate of area A they fill a volume $V=A\cdot L\cdot\cos(30)$. We can estimate the minimum particle diameter by assuming that the molecular conformation is such that they have same packing density as for the flat surface. The volume of the ligand shell should then be the area of the Au core, πd_{core}^2, multiplied by $L\cdot\cos(30)$. Then the minimum diameter is $D_{min}=[d_{core}^3+6\cdot d_{core}^2\cdot L\cdot\cos(30)]^{1/3}$. With these limits, the $Au:C_6S$ particle diameter should be between 2.7 and 3.4 nm, while the $Au:C_{15}S$ particle diameter should be between 3.4 and 5.8 nm.

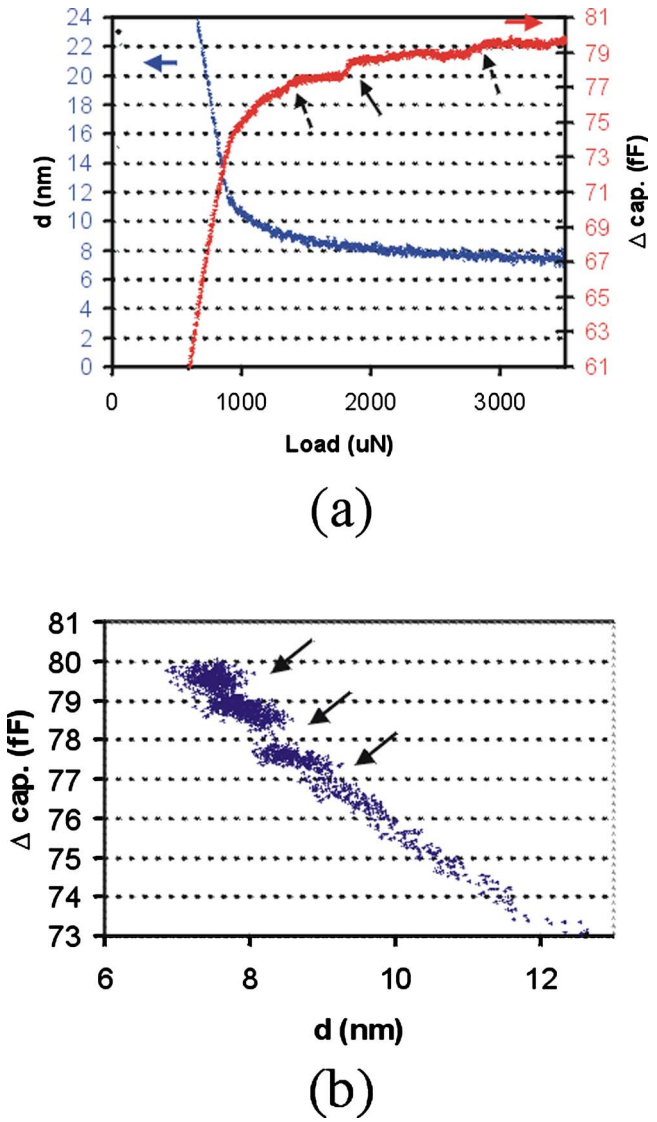

FIG. 3. (Color online) (a) Force-distance and force-capacitance curves for a 3.5 mM suspension of Au:C_6S particles in decane. (b) Distance-capacitance change curve from (a). Capacitance changes (arrows) are observed that are not correlated with changes in the thickness of the confined liquid. This causes breaks in the *d*-*c* curve.

Figure 3(a) shows results for the Au:C_6S suspension. No compressive forces (other than the viscous drag) were observed for d greater than 13 nm. Below 13 nm, the compressive force builds up. The fluid thickness decreased to a stable minimum of about 7 nm, around twice the Au:C_6S particle diameter, at a load of a few mN. No discrete jumps in film thickness were observed.

Surprisingly, a relatively large capacitance jump of $\sim$0.5 fF was observed for $d\sim 8$ nm, along with smaller jumps at $\sim$7.5 and $\sim$9 nm [Fig 3(b)]. Since these jumps were not associated with thickness changes in the film, they must be due to changes in the dielectric properties of the confined suspension layer. When the force ramp was reversed (not shown), the separation increased and the capacitance decreased continuously. In repeated experiments, capacitance jumps are always observed, but the number and

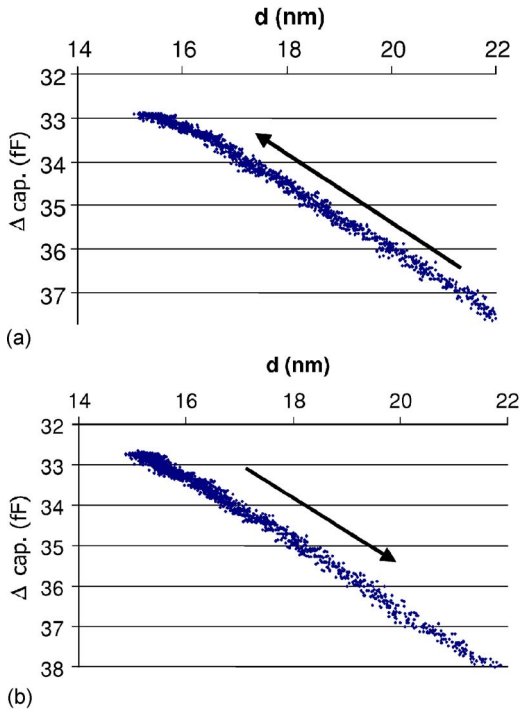

FIG. 4. (Color online) (a) Distance versus capacitance curve for 3.5 mM Au:C_{15}S particles in decane. (b) Similar curve during separation of the surfaces. Steps in capacitance are not observed, unlike the Au:C_6S case.

precise thickness values of the jumps vary from run to run. This is unlike the OCMCTS case, where the number and positions of the layering transitions were reproducible.

Figure 4 shows *C*-*d* plots of a similar experiment for the Au:C_{15}S suspension. No capacitance or thickness jumps were observed in this case. Instead the thickness decreased smoothly, and the capacitance increase was proportional to the thickness decrease. The film thickness at maximum load was 15 nm.

Finally, Fig. 5 shows results for pure decane. Decane has been observed to form layers that were expelled sequentially when confined in a gap of less than 3 nm between parallel surfaces. The step size was 0.5 nm.[29] However, this layered expulsion is not always observed.[30] We did not observe layering transitions with a 2 nm/s approach rate. The transitions were observed, also with steps of $\sim$0.5 nm, when the approach speed was significantly higher, 200 nm/s. This is probably due to the fact that decane is less well ordered than OMCTS under near-equilibrium conditions, so that kinetic effects play a role in decane layering. Viscous forces were detected below $\sim$7 nm, increasing smoothly with decreasing separation until the minimum film thickness of $\sim$1.5 nm was reached. The capacitance changes scaled with separation, as expected for nonpolar molecules.

The fact that no layering transitions were observed in the nanoparticle suspensions is not surprising. To our knowledge layering transitions have never been reported for binary mixtures in either SFA or AFM experiments. The nanoparticles are sufficiently dispersed that layering interactions are unlikely. At the same time they occupy a sufficient volume fraction of the suspension to disrupt decane layering, be-

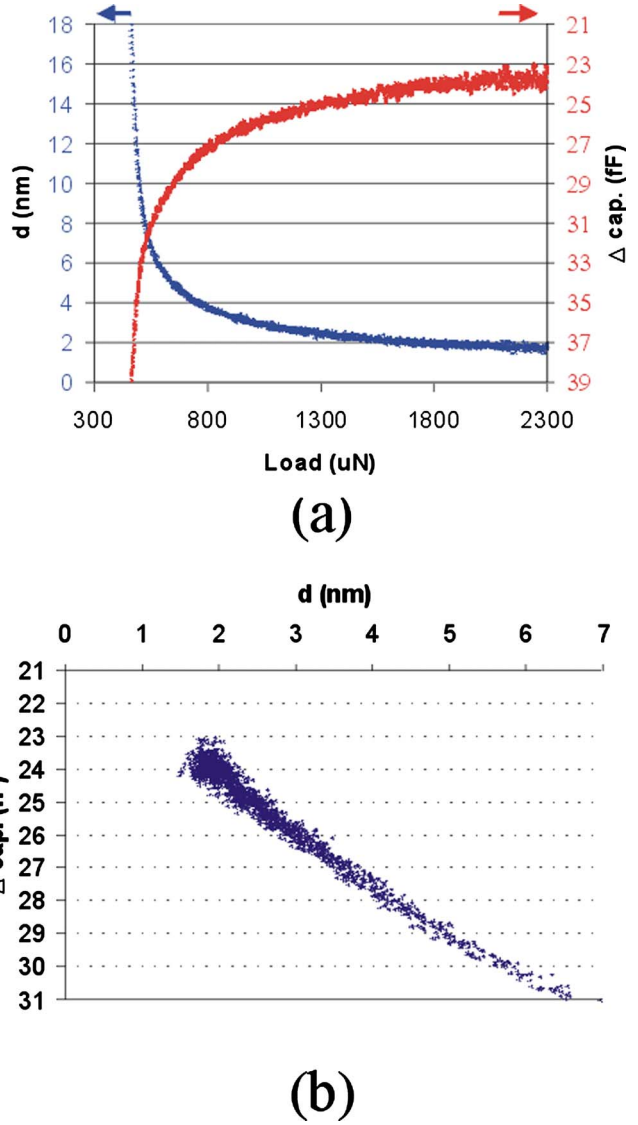

FIG. 5. (Color online) (a) Force-distance and force-capacitance curves for pure decane. (b) The *D-c* curve from (a). No steps in capacitance or separation are observed, and the *d-c* curve is linear.

tween 2.5 and 19% depending on ligand length and conformation.

It is possible that the composition of the confined suspension changes as fluid is squeezed out of the contact, due to some combination of hydrodynamic effects and fluid-mica interactions.[11] As we will see the Au cores of the nanoparticles have a significant van der Waals interaction with the confining mica walls. For a spherical particle near a surface, the interaction energy $U(d)=-rA/6d$, where r is the particle radius, A is the Hamaker constant for particle-solution-mica interactions and d the distance between the surface of the gold cluster and the mica.[17] The Hamaker constant A_{gold} for gold-gold attractions across decane is about 1.95 eV[11] and A_{mica} for mica-mica attractions across decane is 0.069 eV.[17] Then $A_{gold\text{-}mica}$ of gold-mica attractions across decane is calculated to be close to 0.37 eV using $A_{gold\text{-}mica}=\sqrt{A_{gold}A_{mica}}$.[31] For a gold cluster with C_6S ligands in contact with mica, r is 0.9 nm and d is 0.8 nm, giving $U=-69$ meV. Since this interaction energy is larger than kT, it should produce a relatively dense layer of Au particles on the mica surface.

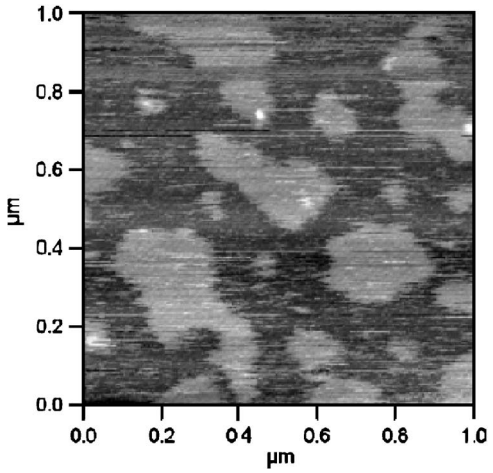

FIG. 6. The contact AFM image of mica dipped into the Au:C_6S suspension then rinsed with pure decane (1 μm$\times$1 μm). Large islands of nanoparticles ~2 nm thick cover about one-third of the surface.

To test this we checked mica surfaces with AFM after dipping for several seconds in the cluster suspension. The surfaces were subsequently rinsed with decane and dried by blowing N_2. We observed large islands, 200 to 300 nm wide and about 2 nm thick covering approximately 1/3 of the surface (Fig. 6). This strongly suggests that a monolayer of clusters is indeed formed on the mica surfaces of our SFA, since it resists rinsing with pure decane. As the thickness of the confined film approaches 3 to 4 times the particle diameter, adsorbed layers of particles hinder drainage of the nanoparticles relative to the decane molecules. This increases the concentration of nanoparticles in the confined fluid at high loads. An increase in concentration would also favor the agglomeration of nanoparticles through mutual van der Waals interactions.

IV. DISCUSSION

The previous results show that the final film thickness of 7 nm for the Au:C_6S suspension (particle diameter 2.8 to 3.4 nm) and 15 nm for the Au:$C_{15}S$ suspension (particle diameter 3.6 to 5.8 nm) is consistent with a layer of particles covering each mica surface and zero to two additional layers trapped between the covered surfaces. The van der Waals interaction will be more important for the C_6 particles, while steric effects are probably more important for the C_{15} particles. Since the capacitance jump of ~0.5 fF for the Au:C_6S is clearly not associated with thickness changes, it must be due to changes in the dielectric properties of the nanoparticle film. The Au cores contribute strongly to the dielectric response, while the effect of the alkane shell is probably similar to that of the decane solvent. The metallic cores will interact through dipole and possibly exchange interactions.[8] Dipole coupling is long range and can be treated classically. Exchange coupling is due to electron tunneling and is therefore very short range. It can play a role

only when clusters are sufficiently close to each other. Let us first consider dipole coupling. For an isotropic two-phase composite medium consisting of spherical metal particles dispersed in a dielectric phase, the effective dielectric constant $\varepsilon_{\text{eff}}(\omega)$ is a function of the volume fraction φ and the distribution of the metallic particles. [8,32] The volume fraction of the Au cores is only 0.0064 in the bulk suspension, which gives $\varepsilon_{\text{eff}} \sim (1+3\varphi)\cdot\varepsilon_f$, where ε_f is the dielectric constant of decane. If decane solvent were completely excluded and the alkanethiol shells were dense φ would have a maximum value of $\sim$0.26 for Au:C_6S and $\sim$0.13 for Au:C_{15}S, resulting in dielectric constants ε_{eff} of $\sim$4.2 and $\sim$3.4, compared to $\sim$2.45 for the bulk suspension.

We can estimate the effect of the change in the volume fraction of the nanoparticles on the capacitance using Eq. (2) and the experimental parameters $a=30\ \mu$m and $D=6.37\ \mu$m. Since the dominant contribution to the capacitance is C_{sphere}, changes in the contact capacitance $C_{contact}$ have a relatively small effect. For the final film thickness of 7 nm, a change in the dielectric constant of the Au:C_6S suspension from 2.45 to 4.2 would give $\Delta C_{contact} \sim 0.04$ fF, and for the final film thickness of 15 nm, a change in the dielectric constant of the Au:C_{15}S suspension from 2.45 to 3.6 would give $\Delta C_{contact} \sim 0.06$ fF. These changes are below the noise level of our experiment, and we can thus exclude classical dipole interactions as the cause of the capacitance jumps observed for the Au:C_6S suspensions.

We propose therefore that the jumps are the result of exchange coupling due to the exponential distance dependence of such coupling. We can regard this as an insulator-to-metal transition, where the clusters are now "electrically connected" to form a metallic slab confined between the mica surfaces. This effectively decreases the "dielectric distance" between the silver electrodes, hence resulting in a stepwise increase in capacitance. Again from Eq. (2), reducing d from $\sim$10 nm to zero gives $\Delta C_{contact} \sim 0.13$ fF. Although still small, this is of the same order as the experimental values (0.5 fF). Multiple capacitance jumps are usually seen in the experiment. They are likely due to inhomogeneous pressure distribution,[33] which brings different parts of the contact into exchange coupling conditions at different times. Also, even outside the flat contact, there is an annular region where the separation between the surfaces is still rather small, for example, it takes $\sim$5 um for d to increase by 1 nm. Some statistical variation in the insulator-to-metal transition process could explain the variation in the number and placement of capacitance jumps.

Strong support for the exchange coupling model lies in the fact that no capacitance jumps were observed for the Au:C_{15}S suspension. With the thicker alkanethiol shells, adjacent cores would still be separated by at least 1.8 nm, too far for an exchange interaction.

V. SUMMARY AND CONCLUSIONS

In summary, combined distance and capacitance measurements in the surface forces apparatus provides a new tool for investigating the organization and interactions of metallic nanoparticles dispersed in suspensions. We demonstrated that capacitance changes due to monolayer layering transitions of nonpolar liquids, such as OMCTS, in the fF range could be measured. This capacitance change is purely due to the geometric effects of electrode proximity. When the method was used to study the confinement properties of metal nanoparticle suspensions, changes in capacitance were observed that have a very different origin. For nanoparticles capped with short alkylthiols (six carbon long chains) capacitance jumps were observed when a few layers of nanoparticles (2 to 3) were trapped between the mica walls. Because no discrete layering transitions were observed, the changes in capacitance were attributed to dielectric changes in the film. We showed that changes due to dipolar coupling between nanoparticles could not explain the magnitude and suddenness of the changes. We also showed that the effect disappear when the same nanoparticles are capped with longer alkylthiols (15 C units). The results strongly support an exchange coupling mechanism mediated by electron tunneling between nanoparticles. Numerical estimations of the expected capacity changes agreed with the measurements within one order of magnitude.

ACKNOWLEDGMENTS

This work was supported by the Director, Office of Energy Research, Office of Basic Energy Sciences, Materials Sciences Division of the U.S. Department of Energy under Contract No. DE-AC02-05CH11231.

*Corresponding author. Email address: mbsalmeron@lbl.gov

[1] M. L. Cohen and W. D. Knight, Phys. Today **43**, 42 (1990).
[2] M. Valden, X. Lai, and D. W. Goodman, Science **281**, 1647 (1998).
[3] P. Crespo, R. Litran, T. C. Rojas, M. Multigner, J. M. de la Fuente, J. C. Sanchez-Lopez, M. A. Garcia, A. Hernando, S. Penades, and A. Fernandez, Phys. Rev. Lett. **93**, 087204 (2004).
[4] A. P. Alivisatos, Science **271**, 933 (1996).
[5] G. Schmid, Chem. Rev. **92**, 1709 (1992).
[6] P. Zhang and T. K. Sham, Phys. Rev. Lett. **90**, 245502 (2003).
[7] Y. Yamamoto, T. Miura, T. Teranishi, M. Miyake, H. Hori, M. Suzuki, N. Kawamura, N. Miyagawa, T. Nakamura, and K. Kobayashi, Phys. Rev. Lett. **93**, 116801 (2004).
[8] J. J. Shiang, J. R. Heath, C. P. Collier, and R. J. Saykally, J. Phys. Chem. B **102**, 3425 (1998).
[9] C. B. Murray, C. R. Kagan, and M. G. Bawendi, Annu. Rev. Mater. Sci. **30**, 545 (2000).
[10] Y. C. Cao, R. Jin, and C. A. Mirkin, Science **297**, 1536 (2002).
[11] B. A. Korgel, S. Fullam, S. Connolly, and D. Fitzmaurice, J. Phys. Chem. B **102**, 8379 (1998).
[12] V. F. Puntes, K. M. Krishnan, and A. P. Alivisatos, Science **291**, 1647 (2001).
[13] C. P. Collier, R. J. Saykally, J. J. Shiang, S. E. Henrichs, and J. R. Heath, Science **277**, 1978 (1997).

[14] G. Markovich, C. P. Collier, and J. R. Heath, Phys. Rev. Lett. **80**, 3807 (1998).
[15] I. S. Weitz, J. L. Sample, R. Ries, E. M. Spain, and J. R. Heath, J. Phys. Chem. B **104**, 4288 (2000).
[16] H. Liu, B. S. Mun, G. Thornton, S. R. Isaacs, Y.-S. Shon, D. F. Ogletree, and M. Salmeron, Phys. Rev. B **72**, 155430 (2005).
[17] J. N. Israelachvili, *Intermolecular and Surface Forces*, 2nd ed. (Acamedic, London, 1992).
[18] P. Franz, F. Wolf, X. D. Xiao, Y. Chen, S. Bosch, and M. Salmeron, Rev. Sci. Instrum. **68**, 2499 (1997).
[19] P. Franz and M. Salmeron, Tribol. Lett. **5**, 151 (1998).
[20] M. Heuberger and M. Zäch, Langmuir **19**, 1943 (2003).
[21] R. G. Horn and D. T. Smith, Appl. Opt. **30**, 59 (1991).
[22] P. Franz, A. Artsyukhovich, R. W. Carpick, and M. Salmeron, Langmuir **13**, 5957 (1997).
[23] P. Franz, N. Agrait, and M. Salmeron, Langmuir **12**, 3289 (1996).
[24] R. G. Horn and J. N. Israelachvili, J. Chem. Phys. **75**, 1400 (1981).
[25] M. J. Hostetler, J. Wingate, C.-J. Zhong, J. E. Harris, R. W. Vachet, M. R. Clark, J. D. Londono, S. J. Green, J. J. Stokes, G. D. Wignall, G. L. Glish, M. D. Porter, N. D. Evans, and R. W. Murray, Langmuir **14**, 17 (1998).
[26] T. Becker and F. Mugele, Phys. Rev. Lett. **91**, 166104–1 (2003).
[27] F. Mugele, S. Baldelli, G. A. Somorjai, and M. Salmeron, J. Phys. Chem. **104**, 3140 (2000).
[28] B. N. J. Persson, *Sliding Friction* (Springer-Verlag, Berlin, 1998).
[29] H. K. Christenson, D. W. R. Gruen, R. G. Horn, and J. N. Israelachvili, J. Chem. Phys. **87**, 1834 (1987).
[30] H. K. Christenson, R. G. Horn, and J. N. Israelachvili, J. Colloid Interface Sci. **103**, 50 (1982).
[31] C. Curran, J. M. Lee, and K. G. Watkins, Opt. Lasers Eng. **38**, 405 (2002).
[32] I. Farbman, O. Levi, and S. Efrima, J. Chem. Phys. **96**, 6477 (1992).
[33] B. N. J. Persson and F. Mugele, J. Phys.: Condens. Matter **16**, R295 (2004).